

# Importance of Polarization and Charge Transfer Effects to Model the Infrared Spectra of Peptides in Solution

Francesca Ingrosso,<sup>\*,†</sup> Gérald Monard,<sup>†</sup> Marwa Hamdi Farag,<sup>‡</sup> Adolfo Bastida,<sup>‡</sup> and Manuel F. Ruiz-López<sup>†</sup>

<sup>†</sup>Equipe de Chimie et Biochimie Théoriques, UMR 7565 SRSMD, CNRS-Nancy Université, BP 70239 Vandœuvre-lès Nancy, France

<sup>‡</sup>Departamento de Química Física, Universidad de Murcia, 30100 Murcia, Spain

## S Supporting Information

**ABSTRACT:** We present a study of the infrared spectrum of N-methyl acetamide (NMA) performed by using molecular dynamics (MD) with a quantum electronic Hamiltonian. A recently developed method, based on the Born–Oppenheimer approximation and on a semiempirical level of quantum chemistry (SEBOMD), is employed. We focus on the solvent effect on the infrared spectrum of the solute, on its geometry, and on its electrostatic properties. We thus run simulations of NMA in the gas phase and in water (64 solvent molecules with periodic boundary conditions), taking into account its two different conformers—cis and trans. The use of a semiempirical electronic Hamiltonian allows us to explore much larger time scales compared to density functional theory based MD for systems of similar size. NMA represents a simple model system for peptide bonds: those infrared bands that are more significant as a signature of the peptide bond (amide I, II, and III and the N–H stretch) are identified, and the solvent shift is evaluated and compared to experiments. We find a satisfying agreement between our model and experimental measurements, not only for the solvent shift but also for the structural and electrostatic properties of the solute. On the other hand, when a molecular mechanics, nonpolarizable force field is used to run MD, very little or nil solvent effect is observed. By analyzing our results, we propose an explanation of this discrepancy by stressing the importance of mutual polarization and charge transfer in an accurate modeling of the solute–solvent interactions.

## 1. INTRODUCTION

Recent advances in computer simulations of the condensed phase have made possible the investigation of dynamics in large systems at a quantum level.<sup>1–8</sup> The use of a quantum Hamiltonian and the definition of the wave function of the whole electronic system result in an accurate description of polarization and charge transfer. This is crucial for modeling bond making/breaking, a feature that is lacking in most molecular dynamics (MD) simulations based on molecular mechanics (MM) force fields. The possibility of treating at a quantum level the electronic Hamiltonian of bio-organic systems in their real environment is thus becoming closer, even for molecular dynamics simulations.

In molecular biology studies, infrared spectroscopy often complements the widely employed X-ray diffraction and NMR techniques, in particular to study proteins and peptides. Amide bands are used to probe the secondary structure when exploring the folding dynamics of proteins.<sup>9,10</sup> A theoretical model of these systems should therefore be able to describe the effect of the environment on the infrared signature of peptide bonds.<sup>11</sup> In addition, theoretical investigations at the DFT-molecular dynamics level have stressed the importance of conformational sampling for an accurate description of specific infrared features, such as, for example, the experimental line shape resulting from a mixture between two different conformations of a peptide.<sup>12,13</sup>

N-methyl acetamide (NMA) has been widely used as a model of the peptide group. It results from a linkage between two residues, a C-terminal (ACE) and a N-terminal (N Met) residue. NMA has two different conformers, corresponding to the cis and trans arrangements of the carbonyl and –NH groups. The trans

form is the most stable in the gas phase and in solution,<sup>14–17</sup> and an experimental evaluation of the energy difference between the two forms in a rigid matrix gives a value of 2.3 kcal/mol,<sup>18</sup> while NMR measurements in 1,2-dichloroethane gave a difference ranging from 2.8 to 3.4 kcal/mol.<sup>19</sup> The free energy barrier between the two forms has been investigated by means of different computational techniques, and it varies between 15 and 20 kcal/mol, depending on the method.<sup>16,20–23</sup> The presence of a solvent enhances the barrier height by 2–3 kcal/mol.<sup>14,20,21</sup>

The literature concerning experimental and theoretical studies of NMA in solution is quite remarkable in size, and it is beyond the scope of this work to provide a full review. We shall only address those works that are closer to our objectives, that is, studies of the IR spectra of NMA in water. The most significant bands in the IR spectrum of a peptide group are the amide I, II, and III bands and the one corresponding to the N–H stretch (Amide A). The amide I mode is mostly related to the C=O stretching motion, which was shown to be coupled with water motions in aqueous solution.<sup>24</sup> Amide II arises mostly from the C–N–H bending motion combined with the C–N stretch, whereas a larger contribution of the C–N stretch combined with the C–N–H bend generates amide III.

The IR spectrum of NMA obtained through classical MM simulations has been compared to the one obtained through a QM/MM approach.<sup>25</sup> The authors have concluded that reliable

Received: January 26, 2011

Published: April 29, 2011

modeling of IR spectra in solution should include the effect of the time-dependent solvent-induced dipole on the solute. The effect of hydrogen bonding with surrounding water molecules on the vibrational frequencies of NMA has been extensively studied by means of quantum chemistry calculations on NMA–water clusters,<sup>26</sup> and it has been described in terms of a spatially inhomogeneous electric field generated by the solvent acting on the solute.<sup>27</sup> Quantum chemistry calculations have been performed on NMA–water clusters (8000 structures) extracted from MM simulations.<sup>28</sup> The results obtained through this approach for the position and for the shape of amide I–III bands are in good agreement with experiments: solute–solvent hydrogen bonding plays a relevant role in reproducing band profiles.

The importance of hydrogen bonding and nonspecific electrostatic interactions between the solute and solvent has been analyzed in depth by modeling the harmonic frequencies and by including anharmonic effects in a joint quantum chemistry and experimental study.<sup>29</sup> Another study based on the interplay between quantum chemistry and experiments has focused on the influence of the environment and the temperature on the amide I band.<sup>30</sup> According to this work, the intensity of this band depends strongly on the solvent, and it varies with temperature. Concerning the solvent effect on the band position, the authors have shown that a simple approach based on the Onsager reaction field can reasonably predict both the solvent-induced and the temperature-induced frequency shifts.

Recent work on theoretical modeling of two-dimensional (2D) IR spectroscopy has been carried out by Jeon and Cho and applied to deuterated NMA in a cluster of 16 D<sub>2</sub>O molecules, based on a QM/MM scheme.<sup>31</sup> The approach has been shown to be successful in reproducing the main features of the experimental 2D IR spectrum. The authors have pointed out that a better description of inhomogeneous broadening might be achieved by including more solvent molecules and by describing them at a quantum level.

Most of the work on IR spectra of small peptides in solution points toward the importance of including polarization and of specific solute–solvent interactions (i.e., hydrogen bonding) in the theoretical description of vibrational properties. In particular, we believe that the mutual polarization between solute and solvent should be included, as well as charge transfer, which might be relevant in the case of NMA, due to the presence of a hydrogen bond donor and of a hydrogen bond acceptor within the peptide bond. All of these terms are taken into account if the electronic Hamiltonian of the full system is treated at the quantum level.

The two conformers of NMA immersed in water, as well as more complex examples of peptides, have already been investigated at the DFT molecular dynamics level, in particular by Gaigeot et al. (see ref 8 for a recent review). However, due to their high computational cost, DFT-based MD simulations are in general limited to simple systems and/or small simulation times. As explained below, the method proposed here is intended to address such limitation by relaxing the level of the quantum chemistry approach used to describe the electronic structure of the solution. This is particularly important when dealing with the calculation of infrared spectra,<sup>25,32</sup> which requires good statistics<sup>33</sup> (as we shall discuss in section 2).

The method used here is based on a semiempirical Born–Oppenheimer molecular dynamics (SEBOMD) approach.<sup>7</sup> At each step of the MD simulation, the electronic wave function of the system is computed with a semiempirical quantum method

making use, if necessary, of a linear scaling algorithm, such as the divide and conquer method.<sup>34,35</sup> Obviously, semiempirical Hamiltonians strongly reduce the computational cost of the simulations compared to *ab initio* or density functional theory based molecular dynamics. The price to be paid is a lower accuracy in the computed molecular properties, though reasonable results are expected for the IR spectra of isolated molecules<sup>36–38</sup>

However, in the case of solvated molecules, further tests are necessary. In fact, traditional semiempirical Hamiltonians, which were parametrized mainly on the basis of gas-phase properties of molecules, do not describe intermolecular interactions correctly. For example, a PM3 Hamiltonian<sup>39</sup> applied to water dimers gives rise to a few wrong features in the potential energy surface.<sup>40,41</sup> In addition, unphysical artifacts are obtained for H–H interactions at short distances.<sup>42</sup> A new parametrization of intermolecular interactions within PM3 has thus been introduced in terms of a parametrizable interaction function (PIF),<sup>40,43</sup> based on fitting high level *ab initio* results. This approach has been tested in depth on liquid water,<sup>7</sup> and though it appears that the average polarizability is slightly underestimated by the semiempirical Hamiltonian, the predicted structure and thermodynamical properties of the liquid (simulation with 216 molecules using periodic boundary conditions, 100 ps time scale) are in good agreement with experimental data. By contrast, the structure of water is not well described by using the standard PM3 Hamiltonian.

The present study illustrates the first application of SEBOMD to study the molecular properties of a solvated solute, and we would like to test the accuracy of this approach to predict the infrared spectrum of biological systems in solution.

This paper is organized as follows. The next section will be devoted to the computational strategies adopted in our study. In section 3, we shall present and illustrate our results, including a comparison with experimental data and other theoretical work in the literature. We shall finally conclude in section 4 by summarizing our findings and by introducing the guidelines of the future developments of our work.

## 2. COMPUTATIONAL DETAILS

In this section, we shall describe in detail the computational methods and the procedures that were adopted to run molecular dynamics simulations and to compute infrared spectra.

First of all, we introduce our MD simulations carried out with a MM force field. We performed MD simulations by using the Amber code, version 9,<sup>44</sup> and the Amber03<sup>45</sup> force field. This force field was recently introduced to overcome some of the shortcomings of previous nonpolarizable force fields in the simulations of proteins in the condensed phase, especially in the prediction of molecular dipole moments and of properties related to the torsional parameters.

Simulations of *cis*- and *trans*-NMA isolated and in cubic boxes containing 64, 125, and 216 SPC/E<sup>46</sup> water molecules were run at 300 K both in the microcanonical ensemble and at constant temperature. In the latter case, the Anderson method<sup>47</sup> was used for temperature control, and the frequency for velocity randomization was 1 ps<sup>−1</sup>. The SPC/E model was used since it gives very similar results to the ones obtained with the semiempirical electronic Hamiltonian and PIF corrections with respect to the structure of liquid water.<sup>7</sup> In addition, SPC/E is one of the best available MM models to describe the dielectric properties (and thus electrostatic solvation properties) of water.<sup>48</sup> We do not expect large effects on the infrared spectrum of NMA due to

using a rigid water model, since the solute–solvent correlations are not included in our calculation (see below).

Simulations in the condensed phase were run with periodic boundary conditions. Long-range electrostatics was treated with the Ewald sum scheme.<sup>49</sup> The size of the boxes was adapted to reproduce the room temperature density of water (0.996 g/mL<sup>50</sup>), by taking into account the volume occupied by the solute.

Equilibration at a constant temperature ( $T = 300$  K, Andersen thermostat) was performed for 500 ps, followed by data acquisition over 1 ns for each simulation. We used a time step of 1 fs. The SHAKE procedure<sup>51,52</sup> was used to keep water molecules rigid, whereas all bonds in the solute molecule were flexible.

Regarding MD simulations with a semiempirical quantum mechanical PM3 Hamiltonian to describe the electronic wave function of the whole system, we compared the results obtained in the gas phase with those obtained in the condensed phase by using the standard PM3 Hamiltonian for intramolecular interactions and the PIF correction for water–water<sup>40,40</sup> and solute–water<sup>42</sup> intermolecular interactions.

We remind the reader that a well-known issue with the PM3 method is an artificial tendency toward pyramidal hybridization of the N atom. A specific correction term (PM3-MM) has thus been introduced to keep peptide bonds planar through a harmonic constraint on the H–N–C–O dihedral. In our calculations, we used the Gaussian 03<sup>53</sup> implementation of this potential. In order to test the effect of this correction on the vibrational frequencies of NMA, we performed gas phase calculations on both the *cis* and the *trans* conformers by carrying out geometry optimization and normal modes analysis in Gaussian.<sup>53</sup> We used both the standard PM3 parameters and the PM3-MM parameters. Other than the different values for the H–N–C–O dihedral and for the molecular dipole moment, no remarkable difference was found in the normal mode frequencies of *cis*- and *trans*-NMA as well as in the interatomic distances.

In water solution, each of the two NMA conformers were dissolved in a box with 64 water molecules, and we ran dynamics on a 300 ps time scale, at the same temperature and using the same time step as in the MM simulations. No SHAKE constraints were applied. Previous equilibration for each MD run was performed over 100 ps starting from a configuration extracted from the molecular mechanics force field MD simulations. The Fock matrix of the system was built at each time step and diagonalized through standard techniques according to the self-consistent field (SCF) scheme. This ensures that the electronic density converges at each step of the simulation, and that the dynamics follows the Born–Oppenheimer potential energy surface.<sup>54,55</sup>

We would like to stress here that the density matrix of the system can also be obtained by means of the divide and conquer approach. However, in our case, the standard diagonalization techniques are faster than the divide and conquer approach, since the size of the system is below the crossover point.<sup>56</sup>

Simulations in the condensed phase were run with periodic boundary conditions, and long-range electrostatic interactions were taken into account by using the Ewald method.<sup>57</sup> The full Fock matrix is built using the minimum image convention for all direct interactions inside the periodic box (direct sum). The Ewald reciprocal sum is incorporated as a correction to the Fock matrix in a way similar to the one proposed by Nam et al:<sup>57</sup> atomic partial charges computed from the semiempirical wave function define an Ewald field in the reciprocal space that can be incorporated in the core Hamiltonian as long as derivatives of

these atomic charges with respect to the density matrix elements are defined. In our implementation, Ewald summation can be performed by using either Mulliken or CM1<sup>58</sup> atomic charges to represent the long-range electrostatic field that self-consistently polarizes the semiempirical wave function.

A typical SCF procedure proceeds as follows: from an initial guess for the density matrix, (1) the atomic charges are computed (Mulliken or CM1 charges); (2) the minimum image Fock matrix is perturbed by the Ewald field (i.e., both the minimum image Fock matrix and the Ewald field are derived from the same density matrix); (3) the total Fock matrix is diagonalized to obtain the wave function coefficients; (4) a new density matrix is built from the coefficients of the molecular orbitals; (5) convergence is checked, and back to step 1 if the procedure has not converged yet.

During the MD simulation, the different sets of charges can be derived from the wave function evaluated at each time step. We also evaluated CM2<sup>59</sup> partial charges. We recall that CM1 and CM2 charges are parametrized to obtain reliable charge-dependent molecular properties, in particular, the molecular dipole moment.

In the case of isolated NMA, we ran simulations in the microcanonical ensemble and at constant temperature (the same conditions as those used for simulations with an MM force field). In all (isolated, condensed phase) simulations, we monitored the O–C–N–H dihedral, in order to make sure that the NMA molecule would stay in the original *cis* or *trans* conformation during the simulation, in agreement with the observation of a high barrier between the two conformers predicted by other calculations.<sup>20–23</sup>

Let us now give some details on the calculation of infrared spectra. It has been shown that the IR absorption line shape  $I(\omega)$  for an isotropic sample is related to the quantum mechanical electrical dipole moment ( $\hat{\mu}$ ) time correlation function (TCF)<sup>60–62</sup> through a Fourier transform (FT) operation:

$$I(\omega) \sim \int_{-\infty}^{+\infty} dt e^{-i\omega t} \frac{\text{Tr}[e^{-\beta\hat{H}} \hat{\mu}(0) \cdot \hat{\mu}(t)]}{\text{Tr}[e^{-\beta\hat{H}}]} \quad (1)$$

where  $\text{Tr}$  denotes the trace operator,  $\hat{H}$  is the Hamiltonian of the system (under the Born–Oppenheimer approximation), and  $\beta$  is the inverse of the Boltzmann constant times the temperature.

In order to make it possible to extend this theory to classical dynamics, one can approximate the quantum TCF by using its classical analog<sup>63</sup> and the quantum electric dipole moment operator by using the classical dipole moment  $\mu$ :

$$I(\omega) \sim Q(\omega) \int_{-\infty}^{+\infty} dt e^{-i\omega t} \langle \mu(0) \cdot \mu(t) \rangle \quad (2)$$

where the effect of approximating quantum operators with their classical counterparts is compensated by the use of the quantum correction factor  $Q$ .

Although different forms for  $Q(\omega)$  have been proposed in the literature,<sup>64</sup> this factor is often omitted, and it has been recently proven that its inclusion does not significantly affect  $I(\omega)$ .<sup>65</sup> We calculate IR spectra by omitting the prefactor, and they are thus expressed in arbitrary units. In addition, we do not introduce any scaling factor to rescale our computed frequencies in order to better reproduce the experimental results.

During the SEBOMD simulation in the gas phase, the dipole moment of NMA can be obtained by applying the dipole moment operator to the wave function of the molecule.



However, the same procedure cannot be applied to NMA in water, due to the delocalization of the wave function over the entire system. This issue has already been discussed in a previous paper,<sup>7</sup> and we adopt here the same approximation proposed there. We evaluate the dipole moment of NMA on the basis of partial atomic charges (instantaneous Mulliken, CM1, and CM2 charges) and instantaneous atomic positions, exactly as it is done for the classical MM simulations. In the gas phase, we compared the SEBOMD results based on partial charges with those obtained from the dipole moment operator. As for the IR spectrum, no differences were observed with respect to the band positions and shape.

In solution, experiments aimed at recording the IR spectrum of a solute use a subtraction method (the spectrum of a blank is subtracted from the spectrum of the full solution). In simulations, this would translate into considering cross-correlations (solute–solvent) to calculate the TCF of the dipole moment as well as solute–solute correlations. However, this approach requires taking into account correlations between solute and solvent motions, and much better statistics are necessary compared to the calculation of self-correlations.<sup>33,66,67</sup> Following the same approximations proposed by Gaigeot and collaborators,<sup>66</sup> we restrict our calculation to self-correlations of the NMA dipole moment.

In the quantum calculation, at each time step, NMA interacts with neighboring water molecules; thus its instantaneous charge may differ from zero. We therefore calculated the dipole moment of NMA with respect to its center of mass.

According to eq 2, we should calculate the Fourier transform of the TCF of the dipole moment. In order to obtain reasonable results, one needs very good statistics for the calculation of the TCF, which means quite long NVE simulations. This can be more easily done in the gas phase. However, when switching to simulations in water with periodic boundary conditions using a semiempirical Hamiltonian, temperature control is necessary. In the Andersen approach, this means that we have NVE intervals between two successive velocity randomizations. In our case, we have a collection of 1 ps NVE simulations over a 300 ps simulation time.

We thus tested a procedure to calculate IR spectra on each 1 ps NVE trajectory, averaging over the 300 1 ps blocks. In the gas phase, we had the chance to compare this procedure with the single 300-ps-long NVE simulation.

Another issue that we analyzed is the numerical method to calculate the Fourier transform of a TCF. In the gas phase, we compared IR spectra obtained by using the Wiener–Khinchin theorem<sup>68</sup> and those obtained by using the maximum entropy method (MEM)<sup>68</sup> with the result obtained by numerically calculating the integral in eq 2.

We found that the MEM and the procedure based on averaging over the 300 NVE blocks, 1-ps-long each, gave spectra in excellent agreement with the direct evaluation of the FT of the dipole TCF in the microcanonical ensemble. The comparison between the different methodologies is available as Supporting Information (SI).

Peak assignment on IR spectra was carried out by using a decomposition of the total vibrational density of states (VDOS) into atomic contributions. This procedure is often used when dealing with peak assignment in calculated IR spectra.<sup>66,67</sup> The VDOS is obtained by calculating the FT of the self-correlation function of the atomic velocities of NMA. The same procedure described above to calculate the FT of a time correlation function

**Table 1.** Geometrical Parameters for Isolated *cis*- and *trans*-NMA<sup>a</sup>

atom	Amber03 <i>cis</i>	Amber03 <i>trans</i>	PM3 <i>cis</i>	PM3 <i>trans</i>
C <sub>ACE</sub> –H <sub>ACE</sub>	1.09	1.09	1.10	1.10
C <sub>NMet</sub> –H <sub>NMet</sub>	1.09	1.09	1.10	1.10
C–O	1.22	1.22	1.22	1.22
N–H	1.01	1.01	1.00	1.00
C <sub>ACE</sub> –C	1.52	1.52	1.51	1.51
C–N	1.33	1.34	1.43	1.43
N–C <sub>NMet</sub>	1.46	1.47	1.47	1.47

<sup>a</sup> Average values from molecular mechanics MD and from SEBOMD with a PM3 Hamiltonian. Distances are in Å. The standard deviation on distances is 0.03 Å with the exception of the CO and CN distances, for which it is 0.02 Å.

was applied. Additionally, some tests were performed by using internal coordinates to confirm the assignment. Results for the VDOS decomposition are provided as SI.

While more precise methods have been proposed to identify the IR bands when the vibrational modes differ significantly from the zero temperature equilibrium normal modes (ENMs) in the gas phase,<sup>69,70</sup> it was not necessary to apply them in the present work, since recent studies have shown that the instantaneous normal modes of the NMA molecule in water solution can be identified using the corresponding ENMs as patterns (see refs 71 and 72).

In the next section, we shall discuss and compare the molecular properties that we obtained from our models. Only IR spectra calculated by applying the MEM on data from NVT simulations will be presented.

### 3. RESULTS

**3.1. Results in the Gas Phase.** We first analyze the average intramolecular properties calculated from our MD simulations. When considering the equilibrium geometry of NMA, no differences in the average bond distances are observed between the *cis* and the *trans* conformers, and the values that we found by using the PM3 Hamiltonian are similar to those found when using the Amber03 force field, with the exception of the C–N distance. Results are collected in Table 1. We recall that PIF parameters only modify the intermolecular (solvent–solvent and solvent–solute) interactions and therefore do not affect the intramolecular properties of NMA in the gas phase.

In Table 2, we report the results obtained for the molecular dipole moment of *cis*- and *trans*-NMA and a comparison with other results obtained with different levels of calculations and from experiments in the literature. Atomic charge parameters for the Amber03 simulations and the Mulliken, CM1, and CM2 charges for the quantum Hamiltonian are provided as Supporting Information.

On average, our PM3 results are in reasonable agreement with the data in the literature; in particular, the result obtained for *trans*-NMA through CM1 charges is in remarkable agreement with experiments.<sup>76,77</sup> The Mulliken charges lead to an underestimation of the molecular dipole moment. Higher levels of quantum chemistry predict a more polar *cis* conformer as well as the PM3 calculations both from the electronic structure calculations on the minimum geometry and from the average value of the SEBOMD simulations. This is in agreement with the trend

**Table 2.** Comparison of NMA Dipole Moment (in Debye) As Obtained from Different Methods in the Gas Phase:

Car–Parrinello Molecular Dynamics (CP-MD), Quantum Chemistry Calculations at the B3LYP/6-31G\* and HF/6-31G(d) Levels of Theory, Our Results for Quantum Calculations at the PM3 Level (in the Case of Standard PM3 Parameters As Well As PM3 with the Correction for the Peptide Bond (PM3-MM)), Our Results from SEBOMD at the PM3 Level (Average Value of the Molecular Dipole—from the Dipole Moment Operator—and the Corresponding Values from Partial Atomic Charges Using Different Schemes), and Our Results from Simulations with the Amber03 Force Field

method	<i>cis</i> -NMA	<i>trans</i> -NMA
CP-MD <sup>66</sup>	4.38	3.99
B3LYP/6-31G* <sup>73</sup>	4.00	3.81
B3LYP/6-311++G* <sup>74</sup>	4.31	3.97
HF/6-31G(d) <sup>75</sup>	4.37	4.22
MP2/6-31G(d) <sup>14</sup>	4.21	4.04
PM3	3.39	3.10
PM3-MM	3.68 (TS) <sup>a</sup>	3.31
PM3-SEBOMD	3.36	3.09
PM3-SEBOMD (Mulliken charges)	3.09	2.64
PM3-SEBOMD (CM1 charges)	3.24	3.79
PM3-SEBOMD (CM2 charges)	3.54	3.54
Amber03 molecular mechanics MD	4.09	4.50
exp. (in benzene) <sup>76</sup>	3.85	
exp. (vapor) <sup>77</sup>	3.71–3.73	

<sup>a</sup> In this case, geometry optimization of the *cis* conformer led to a transition state (TS).

based on Mulliken charges from SEBOMD simulations. On the other hand, the MM force field Amber03 and CM1 charges at a PM3 level predict the *trans* conformer to be more polar than the *cis*. Finally, no difference in polarity is observed when evaluating the molecular dipole moment through CM2 charges.

We now present our results for the IR spectra of *cis*- and *trans*-NMA. In Figure 1, we show the computed spectra for *cis*- and *trans*-NMA as obtained from MM MD simulations by using the Amber03 force field.<sup>45</sup>

The procedure based on the VDOS decomposition, described in section 2, allows us to deduce the following assignment. The bands between 3200 and 3400 cm<sup>−1</sup> are due to the N–H stretch, those between 2800 and 3100 cm<sup>−1</sup> to the C–H stretch (both for the ACE and the N Met residues). The positions of such bands are quite similar for *cis*- and *trans*-NMA, though the former is slightly red-shifted in *trans*-NMA compared to *cis*. On the basis of low temperature nitrogen matrices, the infrared spectra of *cis*- and *trans*-NMA were measured.<sup>18</sup> According to this study, the N–H stretch absorption due to the *cis* form has a peak at 3458 cm<sup>−1</sup> and the one due to the *trans* form at 3498 cm<sup>−1</sup>. Experiments in CCl<sub>4</sub> at ambient temperature found a peak at 3476 cm<sup>−1</sup>, whereas symmetric and antisymmetric C–H stretches fall between 2900 and 3000 cm<sup>−1</sup>.<sup>18,78</sup>

The analysis of the VDOS decomposition shows that in the simulated spectrum of *trans*-NMA the H–N–C bending vibration (amide II) occurs at 1780 cm<sup>−1</sup> and the C–O stretch (amide I) occurs at 1680 cm<sup>−1</sup>, whereas in *cis*-NMA, these two bands superimpose in a broader absorption around 1800 cm<sup>−1</sup>.

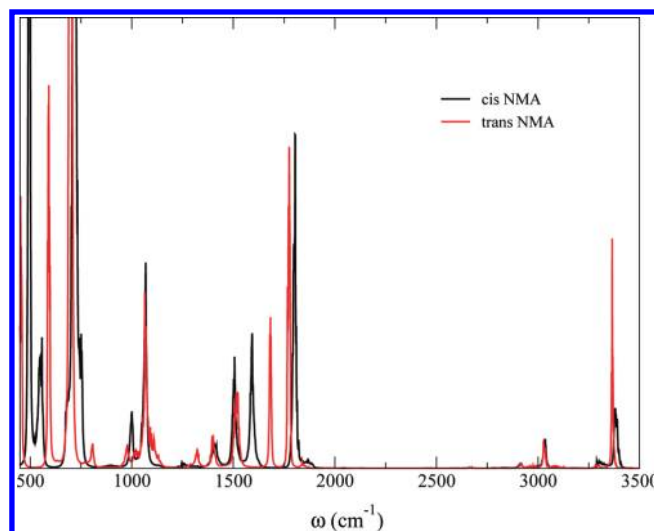


**Figure 1.** Isolated NMA. Calculated infrared spectrum from molecular dynamics simulations with an MM force field. The infrared intensity is arbitrary units.

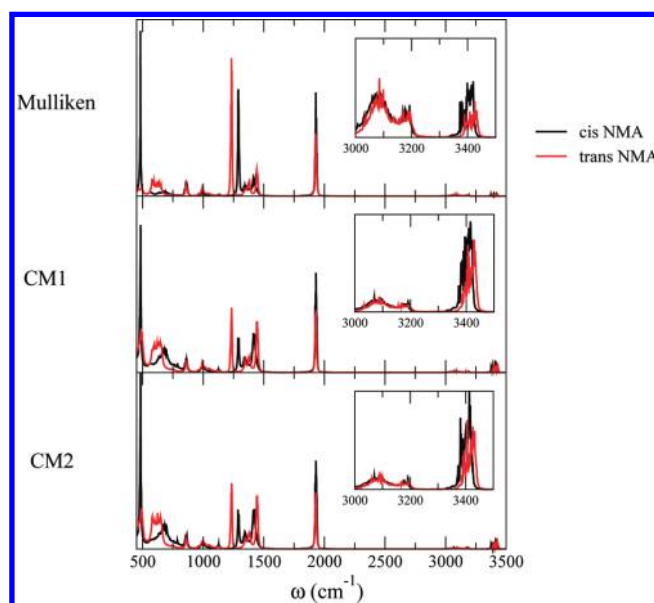


**Figure 2.** Isolated NMA. Calculated infrared spectrum from SEBOMD simulations with a PM3 Hamiltonian. The infrared intensity is arbitrary units.

Experimental measurements of the IR spectrum (see ref 78 and references therein for the *trans* conformer) assign absorption between 1714 and 1731 cm<sup>−1</sup> to amide I and between 1497 and 1500 cm<sup>−1</sup> to amide II. As for the experimental spectrum of the less stable *cis* conformer,<sup>18</sup> the amide I mode occurs in the same frequency range as for the *trans* conformer, while the amide II mode is found at lower frequencies (by about 40 cm<sup>−1</sup>) than in *trans*. In any case, the molecular mechanics force field employed does not give the correct trend between amide I and amide II absorption. It has been pointed out that pyramidalization at the peptide group N atom needs to be taken into account along an MD simulation,<sup>79,80</sup> since the CN torsion and the N–H out-of-plane bending give an important contribution to the NMA IR

**Table 3.** Collection of Results for the Infrared Frequencies Which Are Characteristic of the Peptide Bond of NMA in the Gas Phase and in Water: Amide I (AI), Amide II (AII), Amide III (AIII), and N–H Stretch ( $\delta_{\text{NH}}$ )<sup>a</sup>

mode	Amber03			SEBOMD			experiment <sup>18,78</sup>		
	GP	sol.	$\Delta$	GP	sol.	$\Delta$	GP	sol.	$\Delta$
AI	1680, <sup>b</sup> 1800 <sup>c</sup>	1680, <sup>b</sup> 1800 <sup>c</sup>	0	1920 <sup>b,c</sup>	1800 <sup>b,c</sup>	−120	1714–1731	1625–1646	−90
AII	1780, <sup>b</sup> 1800 <sup>c</sup>	1780, <sup>b</sup> 1800 <sup>c</sup>	0	1420, <sup>b</sup> 1440 <sup>c</sup>	1485, <sup>b</sup> 1522 <sup>c</sup>	75	1497,1500	1565–1585	80
AIII	1250, <sup>b</sup> 1320 <sup>c</sup>	1250, <sup>b</sup> 1330 <sup>c</sup>	5	1290, <sup>b</sup> 1230 <sup>c</sup>	1340, <sup>b</sup> 1370 <sup>c</sup>	95	1255–1259	1314–1317	60
$\delta_{\text{NH}}$	3380, <sup>b</sup> 3370 <sup>c</sup>	3380, <sup>b</sup> 3370 <sup>c</sup>	0	3405, <sup>b</sup> 3410 <sup>c</sup>	3370, <sup>b</sup> 3300 <sup>c</sup>	−110 <sup>c</sup>	3476 <sup>d</sup>	3300	−130

<sup>a</sup> All data in the gas phase (GP), in water (sol.), and the average shift of the condensed phase results with respect to the gas phase ( $\Delta$ ) are reported in  $\text{cm}^{-1}$ . <sup>b</sup> *cis*-NMA. <sup>c</sup> *trans*-NMA. <sup>d</sup> In  $\text{CCl}_4$  solution.

**Table 4.** Geometrical Parameters for *cis*- and *trans*-NMA in Water<sup>a</sup>

atom	Amber03		PM3-PIF	
	Amber03 <i>cis</i>	<i>trans</i>	PM3-PIF <i>cis</i>	<i>trans</i>
$\text{C}_{\text{ACE}}-\text{H}_{\text{ACE}}$	1.09 (0.00)	1.09 (0.00)	1.11 (+0.01)	1.11 (+0.01)
$\text{C}_{\text{NMet}}-\text{H}_{\text{NMet}}$	1.09 (0.00)	1.09 (0.00)	1.11 (+0.01)	1.11 (+0.01)
C–O	1.23 (0.00)	1.23 (0.00)	1.25 (+0.03)	1.25 (+0.03)
N–H	1.01 (0.00)	1.01 (0.00)	1.00 (0.00)	1.01 (−0.01)
$\text{C}_{\text{ACE}}-\text{C}$	1.52 (0.00)	1.52 (0.00)	1.50 (−0.01)	1.51 (0.00)
C–N	1.33 (0.00)	1.33 (−0.01)	1.39 (−0.04)	1.39 (−0.04)
$\text{N}-\text{C}_{\text{NMet}}$	1.46 (0.00)	1.46 (−0.01)	1.48 (+0.01)	1.47 (0.00)

<sup>a</sup> Average values from molecular mechanics MD and from SEBOMD with a PM3 Hamiltonian and PIF corrections. [The standard deviation on distances is 0.03 Å with the exception of the CO and CN distances, for which it is 0.02 Å.] Distances are in Å. In parentheses, we report the shifts with respect to the gas phase.

spectrum. Krimm and collaborators have performed extensive studies showing that including geometry-dependent charges may be more important than developing a polarizable MM force field.<sup>81,82</sup> An alternative approach has been proposed, generally improving the agreement with experiments compared to the classical MM-based evaluation of the vibrational properties of biological systems.<sup>83</sup> This method is based on including additional terms in the potential energy function of the MM force field.

Another band in the IR spectrum from MD simulations, located around  $1590\text{ cm}^{-1}$  in *cis*-NMA, was assigned to the  $\text{H}_{\text{ACE}}-\text{C}_{\text{ACE}}-\text{C}$  bend. This band is red-shifted to about  $1510\text{ cm}^{-1}$  in *trans*-NMA. Between  $1320$  and  $1510\text{ cm}^{-1}$ , in *trans*-NMA we find the amide III bend and the H–C–C and H–C–N bending motions. As for *cis*-NMA, the same bands fall between  $1380$  and  $1590\text{ cm}^{-1}$ . The amide III band position varies between  $1255$  and  $1259\text{ cm}^{-1}$  in experiments, and backbone motions absorb at lower frequencies, where the pattern becomes more and more complicated for both conformers.

In Figure 2, we show the results obtained from SEBOMD simulations by using the PM3 Hamiltonian. We recall that we have different results according to the different scheme for partial atomic charges.

The band positions and their width do not seem to depend on the charge type, which however affects slightly the peak intensities. Results are collected in Table 3.

The two regions in the high frequency portion of the spectrum (between  $3000$  and  $3200\text{ cm}^{-1}$  and around  $3420\text{ cm}^{-1}$ ) are very similar for *cis*- and *trans*-NMA, the latter being blue-shifted by

$20\text{ cm}^{-1}$  compared to the *cis*. This finding is in agreement with the experiment in ref 18.

The amide I band is located for both conformers around  $1920\text{ cm}^{-1}$ . The result is overestimated compared to the average experimental data. The amide II and amide III bands are spread over the  $1230$ – $1480\text{ cm}^{-1}$  region for *trans*-NMA, and in a less extended region (between  $1290$  and  $1480\text{ cm}^{-1}$  region) for *cis*-NMA. The amide II peak in *cis*-NMA is red-shifted by  $20\text{ cm}^{-1}$  compared to the *trans*, again in agreement with the results in ref 18 (red shift of about  $40\text{ cm}^{-1}$ ). The positions of the amide II and amide III bands in the gas phase seem in quite good agreement with experiments. MD simulations within the Car–Parrinello scheme<sup>66</sup> have provided the following results: the frequency for amide I is  $1609\text{ cm}^{-1}$  in *trans*-NMA and  $1606\text{ cm}^{-1}$  in *cis*-NMA. The frequency calculated for amide II is  $1458\text{ cm}^{-1}$  in *trans*- and  $1369\text{ cm}^{-1}$  in *cis*-NMA. Finally, The frequency for amide III is  $1189\text{ cm}^{-1}$  in *trans*- and  $1259\text{ cm}^{-1}$  in *cis*-NMA. Our results are in general agreement with the CPMD results. In particular, the amide I frequency is the same in *cis*- and *trans*-NMA, and the amide II peak in *cis*-NMA is red-shifted compared to *trans*-NMA. However, it seems that the latter approach leads to a better agreement with experiments for the amide I band and to a worse agreement for amide II. In addition, no bands in the N–H stretch region are observed on the basis of CPMD simulations.

In summary, though the amide I experimental band position is not accurately reproduced by our SEBOMD, we obtain a general reasonable agreement with experiments. On the other hand, MD with the Amber03 force field does not reproduce the correct ordering between amide I and II, predicting a lower frequency amide I mode compared to amide II.

**3.2. Results in Water.** First of all, we examine solvent effects on the solute geometry. Compared to the results in the gas phase, few or no differences are observed when using the MM force field, whereas quite a few interesting conclusions can be drawn from an analysis of the results obtained with a quantum electronic Hamiltonian. In the latter case, we used PM3 parameters with PIF corrections, as described in section 2. Results obtained on the intramolecular distances are collected in Table 4.

When going from the gas phase to a solution in water, the C–O bond is elongated. The distance between the C and the N atoms is quite shortened. This is in agreement with the results observed in the literature.<sup>66</sup>

To interpret this result, we recall the two possible resonance structures of NMA in Figure 3.

In a polar solvent, the zwitterionic form is stabilized by electrostatic interactions between the solute and the solvent, and accordingly, the C–O distance elongates and the C–N bond shortens. This effect cannot be reproduced by MM force



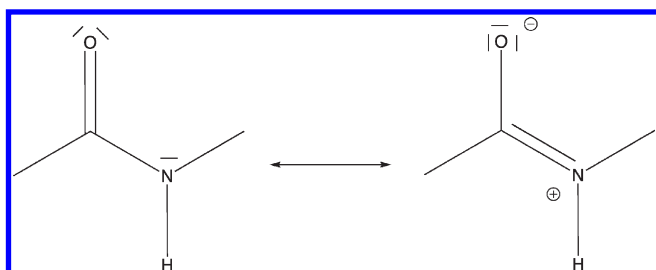


Figure 3. Resonance structures for NMA.

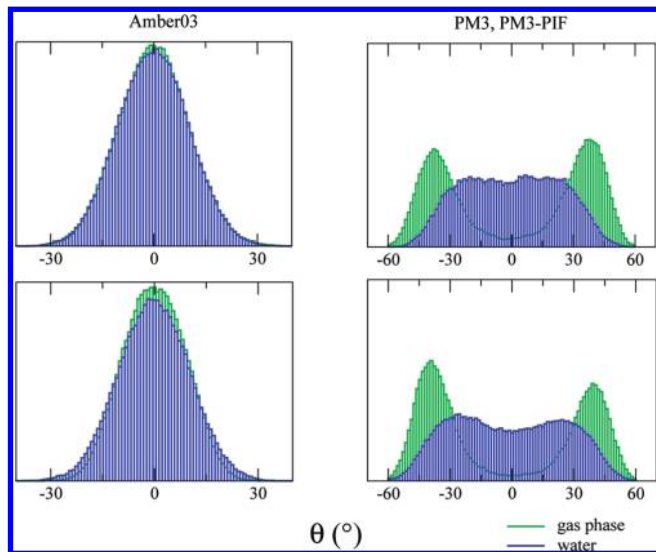


Figure 4. Distribution of the angle formed by the N–H bond with the plane instantaneously identified by N and the two C atoms from molecular dynamics with the Amber 03 force field (left side) and from SEBOMD (right side). Top panels: *cis*-NMA (gas phase and solution). Bottom panels: *trans*-NMA (gas phase and solution).

fields and, not surprisingly, in this case, MD simulations of NMA in water do not predict significant changes in NMA geometry with respect to the gas phase.

As for the out-of-plane position of the N–H bond in the case of simulations with a quantum Hamiltonian, we find distributions corresponding to a pyramidal N atom (see Figure 4).

The distribution is much broader in solution than in the gas phase, and the out-of-plane angle is smaller ( $\pm 16^\circ$  for *cis*- and  $\pm 25^\circ$  for *trans*-NMA). This is consistent with a larger contribution of the zwitterionic resonance structure in a polar solvent.

When analyzing CM1 and CM2 atomic charges (tables collecting all results are available as SI), we observe a displacement of electrons from the –NH group toward the –CO group, again in agreement with a larger contribution of the zwitterionic form. Charges on the O atom decrease, whereas those on the N and the H atoms increase on going from the gas phase to solution. The C atom is less affected. On average, about  $-0.1e$  is transferred from –NH to –CO. We can therefore expect to observe a strong increase of the molecular dipole moment in solution. We collect our results for the molecular dipole moment together with other values obtained at different levels of theory in Table 5.

As in the gas phase, some methods (Car–Parrinello MD, density functional theory with a B3LYP functional and a

Table 5. Comparison of NMA Dipole Moment (in Debye) As Obtained from Different Methods in Aqueous Solution<sup>a</sup>

method	<i>cis</i> -NMA	<i>trans</i> -NMA
CP-MD <sup>66</sup>	7.33 (+2.95)	6.96 (+2.97)
B3LYP/6-31G*-SCRF <sup>73</sup>	4.95 (+0.95)	4.86 (+1.05)
HF/6-31G(d)-RISM <sup>75</sup>	5.79 (+1.42)	5.93 (+1.71)
PM3,PIF(Mulliken)	5.94 (+2.85)	5.41 (+2.77)
PM3,PIF(CM1)	6.26 (+3.02)	6.63 (+2.94)
PM3,PIF(CM2)	6.26 (+2.52)	6.22 (+2.68)
Amber03 MM MD	4.14 (+0.05)	4.54 (+0.04)

<sup>a</sup> Car–Parrinello molecular dynamics (CP-MD), quantum chemistry calculations (B3LYP/6-31G\* in a continuum solvent and HF/6-31G(d) coupled with RISM), our results from SEBOMD at the PM3 and PIF levels (average molecular dipole from partial atomic charges using different schemes), and from simulations with the Amber03 force field. In parentheses, we report the shifts with respect to the gas phase.

6-31G(d) basis set coupled with a continuum solvent, or our PM3 calculation with Mulliken and CM2 charges) predict a more polar *cis* conformer, while others (Hartree–Fock calculations with a 6-31G(d) basis set coupled with a reference interaction site model (RISM) to describe the solvent, molecular mechanics MD with the Amber03 force field, or our PM3 calculation with CM1 charges) predict the *trans* conformer to be the most polar in water.

Not surprisingly, very small induced dipole moments are calculated when running MD simulation with an MM force field. On the contrary, a very large change in the dipole moment on the order of 3 D is calculated from CP-MD and in our simulations when using CM1 charges. The effect is similar when using CM2 charges (about 2.7 D) and Mulliken charges (about 2.7–2.8 D), but much smaller with HF/RISM (1.4–1.7 D) and B3LYP/continuum (about 1 D). Since the two latter methods take into account the solvent as a bulk, specific interactions between solute and solvent are not described explicitly, in particular, the formation of hydrogen bonds with water molecules.

The final part of this section will be devoted to the analysis of the IR spectra in water, and to a comparison with the gas phase results.

The results obtained for the IR spectrum of *cis*- and *trans*-NMA in water when running MD simulations with an MM force field (see Figure 5) show no remarkable differences both in band positions and shapes compared to the gas phase (compare with Figure 1—peak positions are collected in Table 3).

The only perceivable difference in band position involves those modes which are located at lower frequencies (under  $1000\text{ cm}^{-1}$ ), where one can observe some line broadening both for *trans*- and *cis*-NMA.

In addition to the wrong frequency ordering of amide I and amide II bands, the Amber03 force field is thus not able to describe the differences in the IR spectrum of peptides going from the gas phase to aqueous solution.

On the other hand, the results obtained with the SEBOMD approach display significant differences in the condensed phase compared to the gas phase. This finding is in agreement with the CPMD results from ref 66. The effect of the dipole induced by water molecules on the solute has been shown to significantly affect the spectral profile of amide I–III bands.<sup>25</sup> In this work, the authors have compared the relative intensity and the band shape of amide I–III with experiments. An agreement with

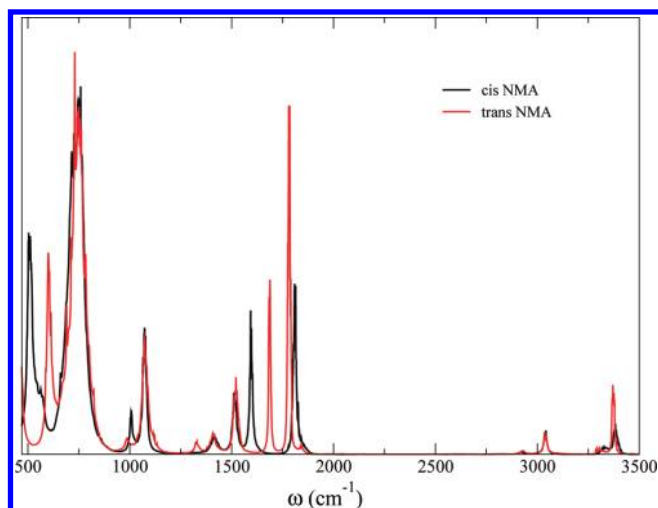


**Figure 5.** NMA in water. Calculated infrared spectrum from MD simulations with an MM force field. The infrared intensity is arbitrary units.

experimental features of these bands is achieved only if the solute is treated at a quantum level by means of a semiempirical electronic Hamiltonian.

In Figure 6, we collect the IR obtained from the three different charge schemes used in this work. When comparing Figure 6 with Figure 2, the IR bands in solution are broadened with respect to gas phase spectra. In addition, differences between spectra for the *cis* and *trans* conformers are enhanced in the condensed phase. A more detailed analysis of solvent effects for each vibrational mode is presented below and summarized in Table 3.

SEBOMD simulations predict the N–H stretch to be red-shifted in both conformers. The *trans* conformer of NMA (band around 3300  $\text{cm}^{-1}$ ) undergoes a larger effect (red shift of about 110  $\text{cm}^{-1}$ ) compared to the *cis* one (band around 3370  $\text{cm}^{-1}$ , shift of about 35  $\text{cm}^{-1}$ ). Experimentally, the frequency of the N–H stretch was measured in  $\text{CCl}_4$  to be 3476  $\text{cm}^{-1}$  and 3300  $\text{cm}^{-1}$  in water.<sup>84</sup> One should point out that this band is very sensitive to temperature and concentration. A large red shift is observed in experiments, the magnitude of which is compatible with our calculated result based on the most stable conformer *trans* NMA.

The band related to the C–H stretch (between 2900 and 3200  $\text{cm}^{-1}$ ) is similar for *cis*- and *trans*-NMA. Compared to the gas phase, this band is quite broadened but not shifted. To our knowledge, no experimental data are available for the frequencies of the C–H stretching motions in aqueous solution.

The amide I band is located around 1800  $\text{cm}^{-1}$ , and the *cis*- and *trans*-NMA conformers are predicted to absorb at the same frequency. In this case, solvent effects lead to a red shift of about 120  $\text{cm}^{-1}$ . Results in the literature for amide I absorption band position vary from 1625 to 1646  $\text{cm}^{-1}$  in aqueous solution.<sup>78</sup> An average red shift of about 90  $\text{cm}^{-1}$  is thus observed, in good agreement with our results.

In the *cis*-NMA spectra, the peak centered at 1485  $\text{cm}^{-1}$  is assigned to the amide II mode. A similar assignment is made in the case of *trans*-NMA for the peak at 1522  $\text{cm}^{-1}$ . Compared to gas phase data, we predict a blue shift of 80  $\text{cm}^{-1}$  in *cis*-NMA and 75  $\text{cm}^{-1}$  in *trans*-NMA. Experimental results for this band in water vary between 1565 and 1585  $\text{cm}^{-1}$ .<sup>78</sup> The average blue shift is thus about 80  $\text{cm}^{-1}$ , again in quite good agreement with our calculated shift.

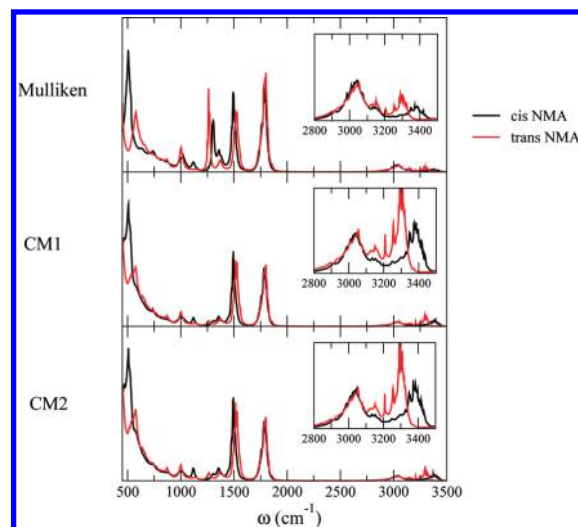


**Figure 6.** NMA in water. Calculated infrared spectrum from SEBOMD simulations with a PM3 Hamiltonian with PIF corrections. The infrared intensity is in arbitrary units.

Bands between 1260 and 1370  $\text{cm}^{-1}$  are quite broadened in solution. In this region, we observe the amide III motion. However, some other modes are active too, and it is not easy to quantitatively extract their position. The *cis* absorption appears at slightly lower frequencies compared to the *trans* form. On average, we can estimate a solvent blue shift effect of about 95  $\text{cm}^{-1}$ . The experimental results for amide III absorption vary between 1314 and 1317  $\text{cm}^{-1}$ , with an average blue shift of 60  $\text{cm}^{-1}$  compared to the gas phase.<sup>78</sup>

The results obtained with Car–Parrinello MD in ref 66 predict an average blue shift of 110  $\text{cm}^{-1}$  for amide I, an average red shift 20 of  $\text{cm}^{-1}$  for amide II, and of 40  $\text{cm}^{-1}$  for amide III. The solvent effect obtained at this level of theory is again in fairly good agreement with our description. A comparison with the AM1/MM method used by Cho and collaborators<sup>25</sup> can only be carried out on the absolute values of the IR frequencies, since the corresponding results in the gas phase are not available. In addition, only the most stable (*trans*) conformer was considered. Amides I, II, and III and the N–H stretch are reported to occur at 1896, 1721, 1444, and 3332  $\text{cm}^{-1}$ , respectively. With the exception of the last band, it seems as if the AM1/MM combined strategy tends to overestimate the frequencies which are characteristic of the peptide bond.

The IR spectrum of *trans* deuterated NMA in a 16  $\text{D}_2\text{O}$  molecule cluster has been calculated on the basis of a PM3/MM approach.<sup>31</sup> If we compare the results obtained in this work with the experimental measurements<sup>78,85</sup> on the amide I' band (the band corresponding to amide I in the deuterated system), we obtain an underestimated blue shift (30  $\text{cm}^{-1}$  in the simulations vs 90  $\text{cm}^{-1}$  in the experiment). Although not conclusive, this comparison suggests that the solvent effect on the position of the solute IR bands is better described when the full system is treated at the quantum level, thus including mutual polarization and charge transfer.

Finally, broad absorption around 1000  $\text{cm}^{-1}$  is related to backbone motion, but it becomes more and more complicated to analyze in depth the lower frequency regions of the spectrum, since many different modes are active there.

Overall, solvent effects are well reproduced by our SEBOMD simulations, although the absolute values of the frequencies are



not predicted with high accuracy. Specifically, when considering the frequency of the amide I, II, and III modes, the calculated frequencies are overestimated, the error being relatively large for amide I but smaller and similar for amides II and III. As a consequence, the gap between the amide I and II frequencies is too high, while the amide II–amide III gap is in reasonable agreement with experiments, both in the gas phase and in solution.

#### 4. CONCLUDING REMARKS

In this paper, we have reported the first analysis of infrared spectra of solvated compounds using molecular dynamics simulations in which the electronic Hamiltonian of the whole solute–solvent system is described by a semiempirical quantum mechanical method. The PM3 Hamiltonian was used to obtain the electronic wave function of the system, and PIF corrections for the core–core interaction terms were considered in order to improve the description of intermolecular interactions. The main scope of this study was to assess the validity of this SEBOMD approach to predict solvent effects on the vibrational frequency of amide bonds. This is an important objective in the perspective of the application of this model to larger systems such as peptides, and eventually proteins.

Overall, our results are quite encouraging. Indeed, a remarkably good agreement was obtained with available experimental data and other calculations in the literature. Interestingly, the same study conducted by using a molecular mechanics, non-polarizable force field showed no remarkable difference in the infrared bands that are more significant signatures of a peptide bond when going from the gas phase to aqueous solution. This finding stresses the importance of a correct description of electronic properties (polarization, charge transfer, etc.) for an adequate molecular modeling of absorption spectra in solution. This is particularly crucial in the case of amide (peptide) bonds since the relative weight of neutral vs zwitterionic tautomeric structures is extremely sensitive to electrostatic interactions with the environment and needs to be accounted for.

As far as the absolute position of the bands is concerned, and not surprisingly, our study shows the usual limitations connected to the use of semiempirical methods, namely on the position of the amide I band. In addition, predicted IR intensities are not quantitative. However, several improvements of the present approach can be envisaged. For instance, including the prefactor in eq 2 might lead to more accurate band shapes,<sup>63,64,86</sup> although a strong effect should not be expected on the bands' intensity.<sup>65</sup> In addition, exploiting the possibility offered by the SEBOMD approach to run long time scale simulations (i.e., compared to ab initio MD) should allow one to unravel the role of the solute–solvent cross-correlation term mentioned in section 2<sup>66</sup> and thus the contribution of intermolecular coupling on the solute vibrations.

Finally, it is worth noting that this approach would be suitable for studying energy transfer in solution. In a recent work, a novel formulation of the instantaneous normal modes (INM) approach was proposed and applied to energy reorganization after the excitation of the amide I<sup>71</sup> and the C–H stretching<sup>72</sup> modes of NMA in solution using an MM, nonpolarizable force field. The relevance of this kind of investigation stems from the importance of energy transfer along peptide chains in biological systems, where polarization and charge transfer effects are expected to play a role in the mechanism of energy redistribution through

intra- and intermolecular modes. Accordingly, coupling the SEBOMD method to the INM analysis is a very promising technique in this domain that will be evaluated in forthcoming work with model peptides.

#### ■ ASSOCIATED CONTENT

**S Supporting Information.** Atomic charges for *cis*- and *trans*-NMA in the gas phase and in solution, a comparison between different methods to calculate the IR spectrum of NMA, a comparison between the results obtained for the NVE and the NVT ensembles, and finally the VDOS for *cis* and *trans* NMA in the gas phase and in solution are given. This information is available free of charge via the Internet at <http://pubs.acs.org>.

#### ■ AUTHOR INFORMATION

##### Corresponding Author

\*E-mail: [Francesca.Ingrosso@cbt.uhp-nancy.fr](mailto:Francesca.Ingrosso@cbt.uhp-nancy.fr).

#### ■ ACKNOWLEDGMENT

This work was partially supported by the Ministerio de Educación y Ciencia of Spain under Projects CTQ2007-66528/BQU and CONSOLIDER CSD2009-00038 and by the Fundación Séneca del Centro de Coordinación de la Investigación de la Región de Murcia under Project 08735/PI/08. M.H.F. gratefully acknowledges a fellowship from the Ministerio de Educación y Ciencia of Spain. F.I., G.M., and M.F.R.L. thank CINES (Montpellier, France) for generous access to their computational facilities.

#### ■ REFERENCES

- (1) Car, R.; Parrinello, M. *Chem. Phys. Lett.* **1985**, *55*, 2471.
- (2) Laasonen, K.; Sprik, M.; Parrinello, M.; Car, R. *J. Chem. Phys.* **1993**, *99*, 9080.
- (3) Carloni, P.; Rothlisberger, U.; Parrinello, M. *Acc. Chem. Res.* **2002**, *35*, 455.
- (4) Silvestrelli, P. L.; Bernasconi, M.; Parrinello, M. *Chem. Phys. Lett.* **1997**, *277*, 478.
- (5) Silvestrelli, P. L.; Parrinello, M. *Phys. Rev. Lett.* **1998**, *81*, 1235.
- (6) Iftimie, R.; Minary, P.; Tuckerman, M. E. *Proc. Natl. Acad. Sci. U. S. A.* **2005**, *102*, 6654.
- (7) Monard, G.; Bernal-Uruchurtu, M. I.; van des Vaart, A.; Merz, K. M., Jr.; Ruiz-López, M. F. *J. Phys. Chem. A* **2005**, *109*, 3425.
- (8) Gaigeot, M. P. *Phys. Chem. Chem. Phys.* **2010**, *12*, 3336.
- (9) Montalvo, G.; Waegle, M. M.; Shandler, S.; Gai, F.; De Grado, W. F. *J. Am. Chem. Soc.* **2010**, *132*, 5616.
- (10) Gilman, R.; Williams, S.; Callender, R. H.; Woodruff, W. H.; Dyer, R. B. *Biochemistry* **1997**, *36*, 15006.
- (11) Schultheis, V.; Reichold, R.; Schropp, B.; Tavan, P. *J. Phys. Chem. B* **2008**, *112*, 12217.
- (12) Gaigeot, M. P. *Phys. Chem. Chem. Phys.* **2010**, *12*, 10198.
- (13) Gaigeot, M. P. *J. Phys. Chem. B* **2009**, *113*, 10059.
- (14) Jorgensen, W. L.; Gao, J. *J. Am. Chem. Soc.* **1988**, *110*, 4212.
- (15) Gao, J.; Freindorf, M. *J. Phys. Chem. A* **1997**, *101*, 3182.
- (16) Villani, V.; Alagona, G.; Ghio, C. *Mol. Eng.* **1999**, *8*, 135.
- (17) Cuevas, G.; Renugopalakrishnan, V.; Madrid, G.; Hagler, A. T. *Phys. Chem. Chem. Phys.* **2002**, *4*, 1490.
- (18) Ataka, S.; Takeuchi, H.; Tasumi, M. *J. Mol. Struct.* **1984**, *113*, 147.
- (19) Drakenberg, T.; Forsen, S. *J. Chem. Soc., Chem. Commun.* **1971**, 1404.
- (20) Luque, F. J.; Orozco, M. *J. Org. Chem.* **1993**, *58*, 6397.

- (21) Mantz, Y. A.; Gerard, H.; Iftimie, R.; Martyna, G. J. *J. Am. Chem. Soc.* **2004**, *126*, 4080.
- (22) Mantz, Y. A.; Gerard, H.; Iftimie, R.; Martyna, G. J. *J. Phys. Chem. B* **2006**, *110*, 13523.
- (23) Mantz, Y. A.; Branduardi, D.; Bussi, G.; Parrinello, M. *J. Phys. Chem. B* **2009**, *113*, 12521.
- (24) Chen, X. C.; Schweitzer-Stenner, R.; Krimm, S.; Mirkin, N. G.; Asher, S. A. *J. Am. Chem. Soc.* **1994**, *116*, 11141.
- (25) Yang, S.; Cho, M. *J. Chem. Phys.* **2005**, *123*, 134503.
- (26) Mennucci, B.; Martinez, J. M. *J. Phys. Chem. B* **2005**, *109*, 9818.
- (27) Hayashi, T.; Zhuang, W.; Mukamel, S. *J. Phys. Chem. A* **2005**, *109*, 9747.
- (28) Besley, N. A. *J. Phys. Chem. A* **2004**, *108*, 10794.
- (29) Andrushchenko, V.; Matějka, P.; Anderson, D. T.; Kaminský, J.; Horncek, J.; Paulson, L. O.; Bouř, P. *J. Phys. Chem. A* **2009**, *113*, 9727.
- (30) Ackels, L.; Stawski, P.; Amunson, K. E.; Kubelka, J. *Vib. Spectrosc.* **2009**, *50*, 2.
- (31) Jeon, J.; Cho, M. *New J. Phys.* **2010**, *12*, 065001.
- (32) Kinnaman, C. S.; Cremeens, M. E.; Romesberg, F. E.; Corcelli, S. A. *J. Am. Chem. Soc.* **2005**, *128*, 13334.
- (33) Richardi, J.; Fries, P.; Millot, C. *J. Mol. Liq.* **2005**, *117*, 3.
- (34) Yang, W.; Lee, T.-S. *J. Chem. Phys.* **1995**, *103*, 5674.
- (35) Dixon, S. L.; Merz, K. M., Jr. *J. Chem. Phys.* **1996**, *104*, 6643.
- (36) Mokrane, A.; Friant-Michel, P.; Cartier, A.; Rivail, J.-L. *THEO-CHEM* **1997**, *395*, 71.
- (37) Li, S.; Schmidt, J. R.; Corcelli, S. A.; Lawrence, C. P.; Skinner, J. L. *J. Chem. Phys.* **2006**, *124*, 2041.
- (38) Garcia-Viloca, M.; Nam, K.; Alhambra, C.; Gao, J. L. *J. Phys. Chem. B* **2004**, *108*, 13501.
- (39) Stewart, J. J. P. *J. Comput. Chem.* **1989**, *10*, 209.
- (40) Bernal-Uruchurtu, M. I.; Martins-Costa, M. T. C.; Millot, C.; Ruiz-López, M. F. *J. Comput. Chem.* **2000**, *21*, 572.
- (41) Csonka, G. I.; Angyan, J. G. *THEOCHEM* **1997**, *393*, 31.
- (42) Harb, W.; Bernal-Uruchurtu, M. I.; Ruiz-López, M. F. *Theor. Chem. Acc.* **2004**, *112*, 204.
- (43) Bernal-Uruchurtu, M. I.; Ruiz-López, M. F. *Chem. Phys. Lett.* **2000**, *330*, 118.
- (44) Case, D. A.; Darden, T. A.; Cheatham, T. E., III; Simmerling, C. L.; Wang, J.; Duke, R. E.; Luo, R.; Merz, J. M. K.; Pearlman, D. A.; Crowley, M.; Walker, R. C.; Zhang, W.; Wang, B.; Hayik, S.; Roitberg, A.; Seabra, G.; Wong, K. F.; Paesani, F.; Wu, X.; Brozell, S.; Tsui, V.; Gohlke, H.; Yang, L.; Tan, C.; Mongan, J.; Hornak, V.; Cui, G.; Beroza, P.; Mathews, D. H.; Schafmeister, C.; Ross, W. S.; Kollman, P. A. *AMBER9*; University of California: San Francisco, 2006.
- (45) Duan, Y.; Wu, C.; Chowdhury, S.; Lee, M. C.; Xiong, G.; Zhang, W.; Yang, R.; Cieplak, P.; Luo, R.; Lee, T.; Caldwell, J.; Wang, J.; Kollman, P. *J. Comput. Chem.* **2003**, *24*, 1999.
- (46) Berendsen, H. J. C.; Grigera, J. R.; Straatsma, T. P. *J. Phys. Chem.* **1987**, *91*, 6269.
- (47) Andersen, H. C. *J. Chem. Phys.* **1980**, *72*, 2384.
- (48) Rami Reddy, M.; Berkowitz, M. *Chem. Phys. Lett.* **1989**, *155*, 173.
- (49) Allen, M. P.; Tildesley, D. J. *Computer Simulation of Liquids*; Oxford University Press: Oxford, U. K., 1987.
- (50) Lemmon, E.; McLinden, M.; Friend, D. *Thermophysical Properties of Fluid Systems. In NIST Chemistry WebBook, NIST Standard Reference Database Number 69*; Linstrom, P. J., Mallard, W. G., Eds.; National Institute of Standards and Technology: Gaithersburg MD, 2008. <http://webbook.nist.gov> (accessed April 2011).
- (51) Ryckaert, J. P.; Ciccotti, G.; Berendsen, H. J. C. *J. Comput. Phys.* **1977**, *23*, 327.
- (52) Ciccotti, G.; Ryckaert, J. P. *Comp. Phys. Rep.* **1986**, *4*, 345.
- (53) Frisch, M. J.; Trucks, G. W.; Schlegel, H. B.; Scuseria, G. E.; Robb, M. A.; Cheeseman, J. R.; Montgomery, J. A., Jr.; Vreven, T.; Kudin, K. N.; Burant, J. C.; Millam, J. M.; Iyengar, S. S.; Tomasi, J.; Barone, V.; Mennucci, B.; Cossi, M.; Scalmani, G.; Rega, N.; Petersson, G. A.; Nakatsuji, H.; Hada, M.; Ehara, M.; Toyota, K.; Fukuda, R.; Hasegawa, J.; Ishida, M.; Nakajima, T.; Honda, Y.; Kitao, O.; Nakai, H.; Klene, M.; Li, X.; Kno, J. E.; Hratchian, H. P.; Cross, J. B.; Adamo, C.; Jaramillo, J.; Gomperts, R.; Stratmann, R. E.; Yazyev, O.; Austin, A. J.; Cammi, R.; Pomelli, C.; Ochterski, J. W.; Ayala, P. Y.; Morokuma, K.; Voth, G. A.; Salvador, P.; Dannenberg, J. J.; Zakrzewski, V. G.; Dapprich, S.; Daniels, A. D.; Strain, M. C.; Farkas, O.; Malick, D. K.; Rabuck, A. D.; Raghavachari, K.; Foresman, J. B.; Ortiz, J. V.; Cui, Q.; Baboul, A. G.; Clifford, S.; Cioslowski, J.; Stefanov, B. B.; Liu, G.; Liashenko, A.; Piskorz, P.; Komaromi, I.; Martin, R. L.; Fox, D. J.; Keith, T.; Al-Laham, M. A.; Peng, C. Y.; Nanayakkara, A.; Challacombe, M.; Gill, P. M. W.; Johnson, B.; Chen, W.; Wong, M. W.; Gonzalez, C.; Pople, J. A. *Gaussian 03*, revision B.03; Gaussian, Inc.: Pittsburgh, PA, 2003.
- (54) Niklasson, A.; Tymczak, C. J.; Challacombe, M. *Phys. Rev. Lett.* **2006**, *97*, 123000.
- (55) Herbert, J. M.; Head-Gordon, M. *Phys. Chem. Chem. Phys.* **2005**, *7*, 3269.
- (56) Goedecker, S. *Rev. Mod. Phys.* **1999**, *71*, 1085.
- (57) Nam, K.; Gao, J.; York, D. M. *J. Chem. Theory Comput.* **2005**, *1*, 2.
- (58) Storer, J. W.; Giesen, D. J.; Cramer, C. J.; Truhlar, D. G. *J. Comput.-Aided Mol. Des.* **1995**, *9*, 87.
- (59) Li, J.; Zhu, T.; Cramer, C. J.; Truhlar, D. G. *J. Phys. Chem. A* **1998**, *102*, 1820.
- (60) Gordon, R. G. *J. Chem. Phys.* **1965**, *43*, 1307.
- (61) Berens, P. H.; Wilson, K. R. *J. Chem. Phys.* **1981**, *74*, 4872.
- (62) McQuarrie, D. A. *Statistical Mechanics*; University Science Books: Sausalito, CA, 2000.
- (63) Schmidt, J. R.; Corcelli, S. A. *J. Chem. Phys.* **2008**, *128*, 184504.
- (64) Egorov, S. A.; Everitt, K. F.; Skinner, J. L. *J. Phys. Chem. A* **1999**, *103*, 9494.
- (65) Lawrence, C. P.; Skinner, J. L. *Proc. Natl. Acad. Sci. U. S. A.* **2005**, *102*, 6720.
- (66) Gaigeot, M. P.; Vuilleumier, R.; Sprik, M.; Borgis, D. *J. Chem. Theory Comput.* **2005**, *1*, 772.
- (67) Gaigeot, M. P.; Sprik, M. *J. Phys. Chem. B* **2003**, *107*, 10344.
- (68) Press, W. H.; Teukolsky, S. A.; Vetterling, W. R.; Flannery, B. P. *Numerical Recipes in Fortran*; Cambridge University Press: Cambridge, U.K., 1992.
- (69) Gaigeot, M. P.; Martinez, M.; Vuilleumier, R. *Mol. Phys.* **2007**, *105*, 2857.
- (70) Martinez, M.; Gaigeot, M. P.; Borgis, D.; Vuilleumier, R. *J. Chem. Phys.* **2006**, *125*, 144106.
- (71) Bastida, A.; Soler, M. A.; Zúñiga, J.; Requena, A.; Kalstein, A.; Fernández-Alberti, S. *J. Chem. Phys.* **2010**, *132*, 224501.
- (72) Bastida, A.; Soler, M. A.; Zúñiga, J.; Requena, A.; Kalstein, A.; Fernández-Alberti, S. *J. Phys. Chem. A* **2010**, *114*, 11450.
- (73) Garcia-Martinez, A.; Teso-Vilar, E.; Garcia-Fraile, A.; Martinez-Ruiz, P. *J. Phys. Chem. A* **2002**, *106*, 4942.
- (74) Han, W. G.; Suhai, S. *J. Phys. Chem.* **1996**, *100*, 3942.
- (75) Du, Q.; Wei, D. *J. Phys. Chem. B* **2003**, *107*, 13463.
- (76) Rodrigo, M. M.; Tarazona, M. P.; Saiz, E. *J. Phys. Chem.* **1986**, *90*, 2236.
- (77) Meighan, R. M.; Cole, R. H. *J. Phys. Chem.* **1964**, *68*, 503.
- (78) Kubelka, J.; Keidel, T. A. *J. Phys. Chem. A* **2001**, *105*, 10922.
- (79) Mannfors, B. E.; Mirkin, N. M.; Palmo, K.; Krimm, S. *J. Phys. Chem. A* **2003**, *207*, 207.
- (80) Mirkin, N. G.; Krimm, S. *J. Phys. Chem. A* **2004**, *108*, 5438.
- (81) Palmo, K.; Krimm, S. *J. Chem. Theory Comput.* **2007**, *3*, 2120.
- (82) Palmo, K.; Mirkin, N. M.; Krimm, S. *Biopolymers* **2003**, *68*, 383.
- (83) Lagant, P.; Nolde, D.; Stote, R.; Vergoten, G.; Karplus, M. *J. Phys. Chem. A* **2004**, *108*, 4019.
- (84) Herrebout, W. A.; Clou, K.; Desseyn, H. O. *J. Phys. Chem. A* **2001**, *105*, 4865.
- (85) Chen, X. G.; Schweitzer-Stenner, R.; Asher, S. A.; Mirkin, N. G.; Krimm, S. *J. Phys. Chem.* **1995**, *99*, 3074.
- (86) Bakker, H. J.; Skinner, J. L. *Chem. Rev.* **2010**, *110*, 1498.